

Evaluation of the proteomic landscape of HPV E7-induced alterations in human keratinocytes reveal therapeutically relevant pathways for cervical cancer

SIVASANGKARY GANDHI¹, MUHAMMAD FAZRIL MOHAMAD RAZIF¹,
SHATRAH OTHMAN^{1,2}, SAJIB CHAKRABORTY³ and NURSHAMIMI NOR RASHID^{1,2}

¹Department of Molecular Medicine, Faculty of Medicine; ²Drug Design and Development Research Group, University of Malaya, 50603 Kuala Lumpur, Malaysia; ³Translational System Biology Laboratory, Department of Biochemistry and Molecular Biology, University of Dhaka, Dhaka 1000, People's Republic of Bangladesh

Received May 25, 2022; Accepted October 18, 2022

DOI: 10.3892/mmr.2023.12933

Abstract. The lack of specific and accurate therapeutic targets poses a challenge in the treatment of cervical cancer (CC). Global proteomics has the potential to characterize the underlying and intricate molecular mechanisms that drive the identification of therapeutic candidates for CC in an unbiased manner. The present study assessed human papillomavirus (HPV)-induced proteomic alterations to identify key cancer hallmark pathways and protein-protein interaction (PPI) networks, which offered the opportunity to evaluate the possibility of using these for targeted therapy in CC. Comparative proteomic profiling of HPV-transfected (HPV16/18 E7), HPV-transformed (CaSki and HeLa) and normal human keratinocyte (HaCaT) cells was performed using the liquid chromatography-tandem mass spectrometry (LC-MS/MS) technique. Both label-free quantification and differential expression analysis were performed to assess differentially regulated proteins in HPV-transformed and -transfected cells. The present study demonstrated that protein expression was upregulated in HPV-transfected cells compared with in HPV-transformed cells. This was probably due to the ectopic expression of E7 protein in the former cell type, in contrast to its constitutive expression in the latter cell type. Subsequent pathway visualization and network construction demonstrated that the upregulated proteins in HPV16/18 E7-transfected cells were predominantly associated with a diverse array of cancer hallmarks, including the mTORC1 signaling pathway, MYC targets V1, hypoxia and glycolysis. Among the various

proteins present in the cancer hallmark enrichment pathways, phosphoglycerate kinase 1 (PGK1) was present across all pathways. Therefore, PGK1 may be considered as a potential biomarker. PPI analysis demonstrated a direct interaction between p130 and polyubiquitin B, which may lead to the degradation of p130 via the ubiquitin-proteasome proteolytic pathway. In summary, elucidation of the key signaling pathways in HPV16/18-transfected and -transformed cells may aid in the design of novel therapeutic strategies for clinical application such as targeted therapy and immunotherapy against cervical cancer.

Introduction

Human papillomavirus (HPV) infections are strongly associated with cervical cancer (CC), and with the incidence of oropharyngeal cancer (1) and anogenital cancer (2). HPV infections are also typically linked to skin or mucosal lesions, such as warts. HPV affects both men and women; however, the disease burden is commonly observed among women due to their high susceptibility for cervical infections (3). Approximately 90% of CC cases are caused by one or more HPV types, particularly HPV16 (detected in ~50% of cases) and HPV18 (detected in 10-15% of cases) (4). HPV16 and -18 are known as high-risk HPV (HR-HPV) subtypes, alongside another 15 types, including HPV31, -33-35, -39, -45, -51, -52, -56, -58, -59, -68, -73 and -82 (5). Usually, HR-HPV infections persist for 1-2 years. Within this period, the virion replicates for months in host tissue with regular transformation, along with active suppression of both innate and adaptive immune responses (6). HPV relies greatly on its potential to control both viral and host gene expression (7). Viral gene transcript regulation is directly related to keratinocyte differentiation in the host (8). Previous studies have reported that HPV-infected keratinocytes exhibit significantly reduced expression of numerous inflammatory mediators (9,10).

HPV is able to promote immune evasion via the expression of oncogenic proteins, which are responsible for the modulation of several immune mechanisms, including antigen presentation and inflammatory pathways (11). HPV E6 and E7

Correspondence to: Dr Nurshamimi Nor Rashid, Department of Molecular Medicine, Faculty of Medicine, University of Malaya, Block F, Jalan Professor Diraja Ungku Aziz, 50603 Kuala Lumpur, Malaysia
E-mail: nurshamimi@um.edu.my

Key words: human papillomavirus, human keratinocytes, E7, proteomics, bioinformatics analysis

oncoproteins support viral oncogenicity as they are expressed concurrently with whole tumor progression and deregulate host cell gene expression (12). Both E6 and E7 proteins exhibit numerous functions; however, they are mainly involved in the inactivation of p53 and retinoblastoma protein (pRb) (13). The inactivation of p53 and pRb can result in the loss of control over DNA damage repair and cell cycle regulation. The E7 oncoprotein binds to and induces degradation of pocket proteins (such as pRb, p107 and p130), which leads to the release of E2F transcription factor family proteins and the expression of S-phase genes (14). However, the suppression of pRb family proteins is not entirely influenced by E7, which suggests that other mechanisms are involved. Furthermore, the degradation of p107 and p130 by E7 is also related to the suppression of DREAM complex-mediated genes (13). Various proteins across different pathways, including activator protein-1 (15), HIF1 (16), krüppel-like factor 4 (17), p73 (18) and other host cell factors have been identified as E7 targets. However, their functional interactions that encourage virus replication and carcinogenesis are not yet fully understood (7).

Understanding the pathogenic mechanisms and signaling pathways associated with HR-HPV, along with the identification of differentially expressed protein-protein interactions (PPIs), could aid in the design of novel therapeutic strategies that target HPV-associated CC. Therefore, the present study evaluated changes in protein expression levels between normal human keratinocytes (HaCaT) transfected with recombinant HPV16/18 E7 and HPV-transformed cells (Caski and HeLa) to identify proteins that may contribute to cancer hallmark enrichment. Deciphering alterations in cellular protein interactions and their associated pathways during the viral life cycle is essential to understand the evolution of HPV E7 function in cervical carcinogenesis.

Materials and methods

Cell lines. Human HaCaT keratinocyte cells (Addexbio Technologies), HPV16-positive CC CaSki (passage 9) and HPV18-positive CC HeLa (passage 11) cell lines (both from the Laboratory of Virology, Department of Medical Microbiology, University of Malaya, Kuala Lumpur, Malaysia), were used in the present study. The HaCaT cells were authenticated using STR profiling. CaSki cells carry integrated viral HPV16 DNA. HeLa cells contain integrated viral HPV18 DNA. All cell lines were maintained in T25 flasks with 5 ml Dulbecco's Modified Eagle's Medium (Gibco; Thermo Fisher Scientific, Inc.), 10% heat-inactivated fetal bovine serum (Gibco; Thermo Fisher Scientific, Inc.) and 1% penicillin/streptomycin (Gibco; Thermo Fisher Scientific, Inc.). Cells were maintained under standard incubation conditions of 10% CO₂ with 95% humidity at 37°C.

Transfection of HPV16/HPV18 E7 recombinant plasmids in human keratinocytes. Transfection of HaCaT cells was performed according to the manufacturer's protocol. Briefly, FuGENE® HD transfection buffer (Promega Corporation) was added to 2 µg of each plasmid [pMSCVpuro; Addgene (Fig. S1) (control); pMSCVpuro-HPV16E7; and pMSCVpuro-HPV18E7], which were diluted in 100 µl serum-free Opti-MEM™ Reduced Serum medium (Gibco; Thermo Fisher

Scientific, Inc.). Subsequently, 100 µl transfection mixture containing 2 µg of the nucleic acid was added to HaCaT cells (3x10⁵) grown in a 6-well plate and incubated at 37°C for 48 h. The cells were then washed and maintained using 0.5 µg/ml puromycin (Gibco; Thermo Fisher Scientific, Inc.) for 24 h post-transfection and incubated for a further 48 h to establish stable transformants before harvesting. Transfection efficiency was assessed using reverse transcription-quantitative PCR (RT-qPCR) and the results are presented in Fig. S2.

RNA extraction and RT-qPCR. Total RNA was extracted using the FavorPrep™ Blood/Cultured Cell Total RNA Mini Kit (Favorgen). The cDNA was prepared using the RevertAid™ First Strand cDNA Synthesis Kit (Thermo Fisher Scientific, Inc.) according to the manufacturer's protocol. qPCR was performed using Absolute SYBR Green ROX (Thermo Fisher Scientific, Inc.) in triplicate using an ABI PRISM™ 7900HT sequence detector (Applied Biosystems; Thermo Fisher Scientific, Inc.) (19). The primers used for the qPCR reactions are presented in Table SI. PCR was performed under the following thermocycling conditions: 95°C for 15 min, followed by 40 cycles at 95°C for 15 sec, 58°C for 30 sec and 72°C for 30 sec. Optimization was performed for each primer set and the relative quantification was performed with normalization against β-actin (20).

Protein extraction and quantification. Proteins were extracted using RIPA lysis buffer [NaCl, 150 mM; 1% Triton X-100; Tris-HCl, 50mM (pH, 8.0); 0.5% sodium deoxycholate; 0.1% SDS; Halt™ Protease Inhibitor Cocktail (100X; Thermo Fisher Scientific, Inc.)]. Cells were washed twice with ice-cold PBS and mixed with ice-cold RIPA lysis buffer. The cell lysate was centrifuged at 13,000 x g for 20 min at 4°C. The supernatant, containing soluble proteins, was collected and stored at -80°C until further analysis. The concentration of the extracted proteins was determined using the Bradford assay (21). Bovine serum albumin (MilliporeSigma) was used as a protein standard to construct the calibration curve.

In-solution tryptic digestion and desalting. A total of ~500 µg protein from each sample were digested in 50 mM ammonium bicarbonate digestion buffer together with 100 mM DTT reducing buffer and incubated at 95°C for 5 min. The samples were cooled to ambient temperature and alkylated in 100 mM iodoacetamide buffer for 20 min in the dark. Trypsin is a serine protease that is highly specific, digesting protein into peptides by cutting at the carboxyl side of arginine and lysine residues. Samples were then incubated with trypsin (Promega Corp.) at 37°C for 3 h and another 1 µl trypsin was added for overnight incubation at 30°C. The digested peptides were desalted, lyophilized and stored at -80°C until further experimentation (22).

Protein identification using nano-electrospray ionization-liquid chromatography-tandem mass spectrometry (nano-ESI-LC-MS/MS). Protein identification using nano-ESI-LC-MS/MS was performed with certain modifications (23). Trypsin-digested peptides (500 µg) were loaded onto a 300 Å, SB-C18, 160 nl enrichment column and 75 µm x 150 mm analytical column (cat. no. G4240-62010;

Agilent Technologies, Inc.) with a flow rate of 4 $\mu\text{l}/\text{min}$ using a capillary pump and 0.5 $\mu\text{l}/\text{min}$ using an Agilent 1200 nano pump. The eluted peptides were subjected to nano-ESI MS/MS using an Agilent 1200 Series HPLC-Chip/MS System Interface, coupled with the Agilent 6550 Q-TOF LC/MS system (Agilent Technologies, Inc.). Injection volume was adjusted to 1 $\mu\text{l}/\text{sample}$. The mobile phases were 0.1% formic acid in water (solution A) and 90% acetonitrile with 0.1% formic acid (solution B) for 4 min and 70% solution B for 3 min, using an Agilent 1200 Series nanoflow LC pump. Ion polarity was set to positive ionization mode, the drying gas flow rate was 5.0 $\mu\text{l}/\text{min}$ and the temperature was fixed at 325°C. The fragmentor and capillary voltage were set at 360 and 1,900 V, respectively. The spectra were acquired in MS/MS mode with an MS scan range of 110–3,000 m/z and MS/MS scan range of 50–3,000 m/z. Precursor charge selection was set as a double-, triple- or more than triple-charged state, with the exclusion of precursors 1,221.9906 m/z ($z=1$) set as reference ions. Data were extracted using MH^+ (positive ion) mass range between 50–3,200 Da and processed using the Agilent Spectrum Mill MS Proteomics Workbench software packages version B.04.00 (Agilent Technologies, Inc.). The raw data files obtained from the LC-MS/MS were processed using PEAKS DB analysis to evaluate the relative protein abundance.

De novo identification of peptides using PEAKS Studio 7.0. PEAKS DB is a proteomic software package for MS/MS designed for peptide sequencing, protein identification and quantification (24). Peptide identification was performed using automated *de novo* sequencing in PEAKS Studio 7.0 (Bioinformatics Solution, Inc.) (25). Proteins were identified from HPV-transfected and -transformed cells using the Uniprot *Homo sapiens*, type Swissprot and Trembl databases, processed with PEAKS 7.0 (Bioinformatics Solution, Inc.) and carbamidomethylation was set as a fixed modification. Subsequently, high-confidence proteins were identified by setting a false discovery rate (FDR) threshold of 1%, unique peptide ≥ 1 and $-10\lg P > 20$.

Label-free quantification (LFQ). Label-free mass spectrometry-based quantitative approaches provide powerful, fast and low-cost tools for analyzing protein changes in complex biological samples in several large-scale biomarker discovery studies (26). However, to avoid any variation errors in the performance of LC and MS, a carefully controlled normalization step is required. LFQ was performed using PEAKS studio 7.0 (Bioinformatics Solution, Inc.) the abundance of proteins was calculated using normalized spectral protein intensity (LFQ intensity), in which proteins were quantified by comparing the number of identified MS/MS spectra from the same protein in each of the multiple LC-MS/MS data sets. It is possible that an increase in protein abundance results in a higher number of proteolytic peptides and vice versa. In turn, a larger number of proteolytic peptides leads to higher protein sequence coverage and increased number of both identified unique peptides and total MS/MS spectra (spectral count) for each protein (27). HaCaT-pMSCV puro was used as a control to normalize the LFQ of fold changes for significant proteins. The pheatmap package was used to present differentially expressed proteins with hierarchical clustering.

Data acquisition and statistical analysis. Three biological replicates for each cell line, including the control, underwent LC-MS/MS. P-values were obtained using the Benjamini-Hochberg FDR. Statistical analysis was performed using GraphPad Prism version 5.0.0 for Windows (GraphPad Software, Inc.) and the data are presented as the mean \pm standard deviation (SD). A comparison between the transfected samples and control was conducted using Student's t-test, and $P < 0.05$ was considered to indicate a statistically significant difference.

Bioinformatics analysis

UpSet plot analysis. An UpSet plot is commonly applied to visualize a dataset with more than three overlapping patterns. It is similar to a Venn diagram but more comprehensive (28). An UpSet plot (<https://upset.app/>) for HaCaT control, HaCaT-16 E7, HaCaT-18 E7, CaSki and HeLa datasets was generated to identify unique and overlapping proteins across all five cell lines.

Volcano plot analysis. The identified proteins were further analyzed using Perseus (version 1.5.3.0) (29) for differential expression analysis. Firstly, the reverse, site-only and contaminant peptides were removed from the dataset, with missing values input using a normal distribution. This analysis identified significant protein changes using Student's t-test with an $\text{FDR} < 0.05$ between HPV-transfected and HPV-transformed cells. The data were presented using a volcano plot, where the x-axis represented the fold change and the y-axis presented the $-\log P$ -value.

Molecular signature database (MSigDB) analysis. The MSigDB (30) is one of the largest and most popular repositories of gene sets for use with the Gene Set Enrichment Analysis (GSEA) software tool. The GSEA tool was used to characterize protein expression levels in HaCaT control and HPV-transfected cells with the accession no. MSV000090470 (massive.ucsd.edu). The cancer hallmarks for upregulated proteins in HPV-transfected cells were also identified (31). The P-value summary was used to determine the FDR according to the method described by Benjamini (32). The proteins were identified for each cancer hallmark, sorted by their P-value and FDR values. The top-scoring protein with a summary $\text{FDR} < 0.01$ was considered to encompass the definitive cancer hallmark set.

PPI network. Cytoscape 3.8.2 is a freely available platform for network visualization and analysis (Cytoscape_v3.8.2). PPI network construction in Cytoscape requires each protein in the input file to have the same identifiers. Therefore, UniProt ID mapping with Cytoscape was applied to standardize the identifiers. All upregulated proteins in HPV-transfected cells were selected to create a PPI network. The interactors in the network were carefully evaluated to identify potential interactions between the nodes.

Search Tools for the Retrieval of Interacting Genes (STRING) functional enrichment analysis. Gene Ontology (GO) enrichment analysis was applied to identify the function of differentially expressed proteins based on three main aspects as follows: i) Molecular function (MF); ii) cellular component (CC); and iii) biological process (BP) in which they were mutually involved. The list of identified proteins was evaluated using version 10 of the STRING database

(<http://string10.embl.de>) to predict the identified proteins. The interaction score was set to a high confidence level of 0.700. GO terms with FDR<0.01 were defined as the enriched terms for the differentially expressed proteins; *Homo sapiens* was selected as the organism.

Results

Protein identification in HPV-transfected and -transformed cells. Protein profiling analysis was performed using total protein fractions from each cell type to identify differentially expressed proteins in HPV-transfected human keratinocytes (HaCaT-HPV16/18 E7) and HPV-transformed cells (CaSki and HeLa), with empty vector pMSCV-puro human keratinocytes (HaCaT) used as a control. After quality control assessment of each protein, including average mass, number of peptides and number of uniquely expressed peptides, high confidence proteins (-10lgP>20 considered significant) were identified. A total of 41 proteins were identified in HaCaT cells (Table SII), 29 proteins were identified in HaCaT-pMSCVpuro (control) cells (Table SIII), 85 proteins were identified in HaCaT-HPV16 E7 cells (Table SIV) and 104 proteins were identified in HaCaT-HPV18 E7 cells (Table SV). For HPV-transformed cells, 45 and 39 proteins were identified in CaSki (Table SVI) and HeLa (Table SVII) cells, respectively. The results of the present study demonstrated that glucose-6-phosphate isomerase (GPI) and fructose-bisphosphate aldolase (ALDOA) were the two common proteins among the cell lines. GAPDH, tubulin α -1A chain (TUBA1A), tubulin α chain, heat shock 70kDa protein 8 isoform 2 variant (HSPA8), profilin (PFN1), keratin type I cytoskeletal 17, annexin 5, transketolase, annexin 2 (ANXA2), keratin type II cytoskeletal 8 (KRT8) and peroxiredoxin-1 (PRDX1) were identified in CaSki and HeLa cells. Tubulin α -1B chain and elongation factor 2 (EEF2) were common proteins identified in HaCaT-HPV16/18 E7, CaSki and HeLa cells.

LFQ and heat map clustering analysis between HPV-transfected and -transformed cells. The high-confidence proteins (P=0.01) were identified across HPV-transfected and -transformed cells were subjected to LFQ to assess the differentially expressed proteins with significant fold changes (Table SVIII). HaCaT control cells were used for normalization. A total of 62 differentially expressed proteins were identified. A heat map of differentially expressed proteins was generated with legend color bar, column and row annotations (Fig. 1). All proteins were subsequently grouped based on the hierarchical clustering between HPV-transfected and -transformed cells. The upregulated proteins were clustered at the top of the heat map (blue), whereas the downregulated proteins were clustered at the bottom (red). The results of the present study identified 37 upregulated and 13 down-regulated proteins. The hierarchical clustering (column) of HPV-transfected cells demonstrated more proteins in common between HaCaT-HPV16 E7 and HaCaT-HPV18 E7 cells compared with those identified in both HPV-transformed cells. Furthermore, hierarchical clustering (row) resulted in two distinct clusters, separated by upregulated and downregulated proteins based on assessed fold change. Most proteins in HPV-transfected cells were upregulated. EIF4A1, PFN1,

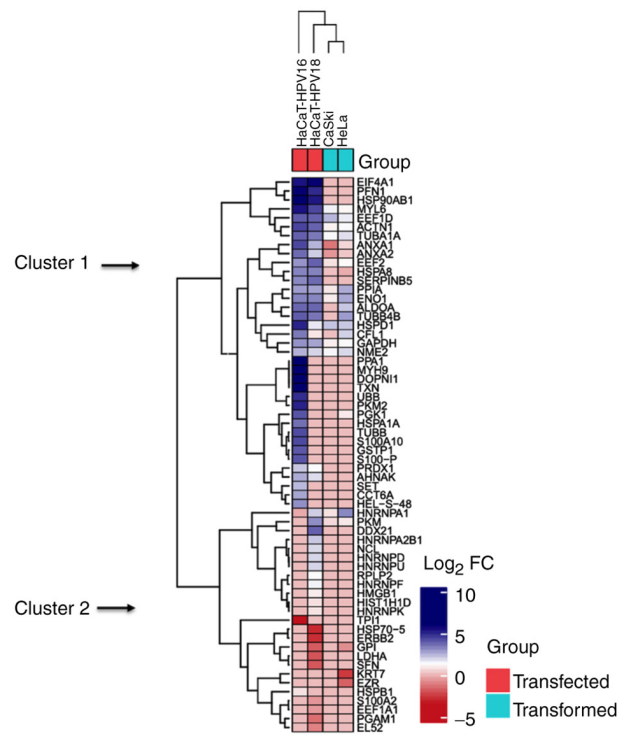


Figure 1. Heat map presentation of the relative protein expression levels (log₂FC) for 62 proteins compared with HaCaT cells. The columns represent the HPV-transformed and -transfected cell lines, and rows indicate the proteins. The color-coded intensities represent the expression level of each protein. The upregulated and downregulated proteins are presented in blue and red, respectively. FC, fold change; HPV, human papillomavirus.

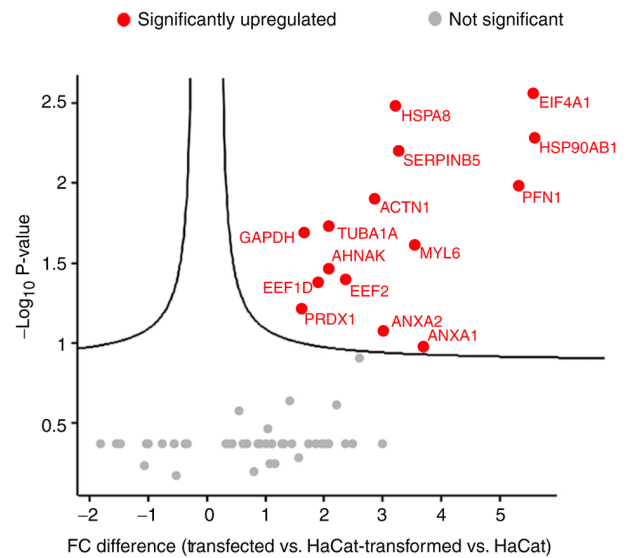


Figure 2. Volcano plot of the 62 differentially expressed proteins in human papillomavirus-transfected and -transformed cells vs. the HaCaT control. The y-axis presents the mean expression value [-log(P-value)] and the x-axis presents the FC difference. Red dots represent significantly differentially expressed proteins (P<0.05). Grey dots represent differentially expressed proteins that did not reach statistical significance (P>0.05). FC, fold change.

HSP90AB1, MYL6, EEF1D, ACTN1, TUBA1A, ANXA1, ANXA2, EEF2, HSPA8, SERPINB5, PPIA, ENO1, ALSOA, TUBB4B, HSPD1, CFL1, GAPDH, NME2, PPA1, MYH9, DOPNI1, TXN, UBB, PKM2, PGK1, HSPA1A, TUBB,

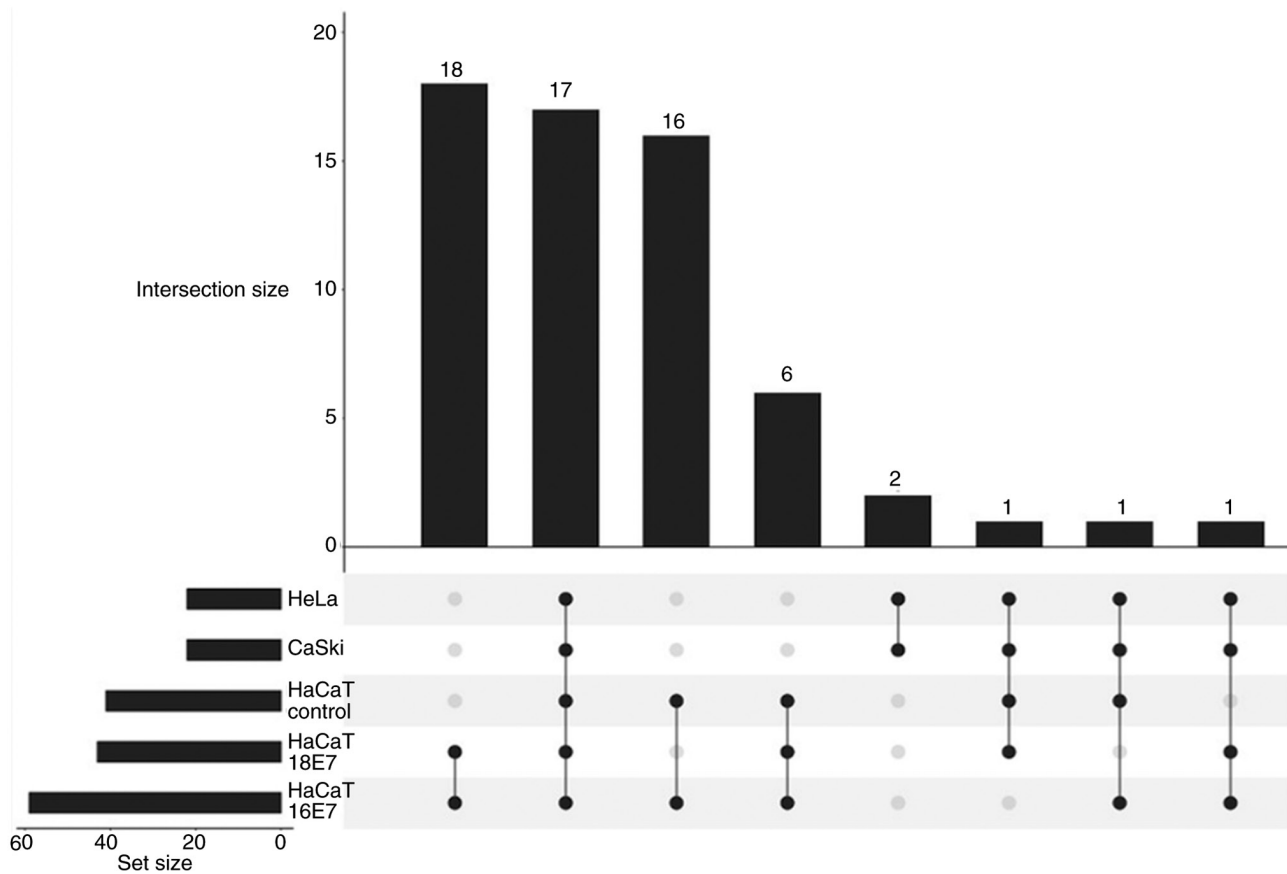


Figure 3. UpSet intersection plot based on protein linkages between HaCaT (control), HPV-transfected (HaCaT-HPV16 E7 and HaCaT-HPV18 E7) and HPV-transformed (CaSki and HeLa) cells. Horizontal bars represent the number of protein linkages identified in each cell line. Vertical bars represent the number of protein linkages present between the cell lines. Dots indicate cell lines in which the proteins were identified. HPV human papillomavirus.

S100A10, GSTP1, S100-P, PRDX1, AHNAK, SET, CCT6A and HEL-S-48 were upregulated in HPV-transfected cells compared with in both HaCaT (control) and HPV-transformed cells (Cluster 1). However, Cluster 2 demonstrated a mixed pattern with both upregulated and downregulated proteins. The upregulated proteins in Cluster 2 were HNRNPA1, PKM, DDX21, HNRNPA2B1, NCL, HNRNPD, HNRNPU, RPLP2, HNRNPF, HMGB1, HIST1H1D, HNRNPK and TPI1. The downregulated proteins were HSP70-5, ERBB2, GPI, LDHA, SFN, KRT7, EZR, HSPB1, S100A2, EEF1A1, PGAM1 and EL52.

Volcano plot of proteins with significantly increased expression levels in HPV-transfected and -transformed cells.

Proteins in the aforementioned heat map analysis (Fig. 1) were further analyzed using a volcano plot to assess the proteins with the most significantly increased protein expression levels in HPV-transfected and -transformed cells (Fig. 2). The volcano plot presented fold-change differences and protein expression level distribution in HPV-transfected cells vs. HaCaT cells, and in HPV-transformed cells vs. HaCaT cells. Proteins were presented in graphs according to fold change (difference) and significance ($-\log_{10}$ P-value). The 15 upregulated proteins mainly observed in HPV-transfected cells were GAPDH, EEF1D, PRDX1, TUBA1A, AHNAK, EEF2, ANXA2, ANXA1, ACTN1, MYL6, SERPINB5, HSPA8, EIF4A1, HSP90AB1 and PFN1. Among these proteins,

EIF4A1, HSP90AB1, HSPA8 and SERPINB5 were presented toward the top right of the plot, which indicated high statistical significance and fold change. EIF4A1 serves a crucial role in the transformation and progression of various types of cancer as it is part of the EIF4F complex that controls initiation rates of pro-oncogenic mRNAs involving the PI3K/Akt/mTOR signaling pathway (33). HSP90AB1, a chaperone protein, is often upregulated in cancerous cells and it is able to stabilize their protein functions with activating mutation (34). HSPA8 is a member of the HSP70 family, which collectively functions as a buffering system for cellular stress which is required for cancer cell survival (35). Fold-change differences in the expression levels of the remaining proteins were not statistically significant.

UpSet intersection plot of HPV-transfected and -transformed cells.

The total number of quantified proteins in HaCaT control, HPV-transfected (HaCaT-HPV16 E7 and HaCaT-HPV18 E7) and HPV-transformed (CaSki and HeLa) cells were further evaluated using UpSet plot analysis (Fig. 3). The UpSet intersection plot was presented as a matrix layout to visualize overlaps and differences between qualified proteins across all five cell lines. Dark circles in the matrix indicate sets that are part of the intersection. A high number of linkages indicate a marked association of proteins between the respective cell lines (36). A total of 18 protein linkages were demonstrated between HaCaT-HPV16 E7 and HaCaT-HPV18 E7 cells, the

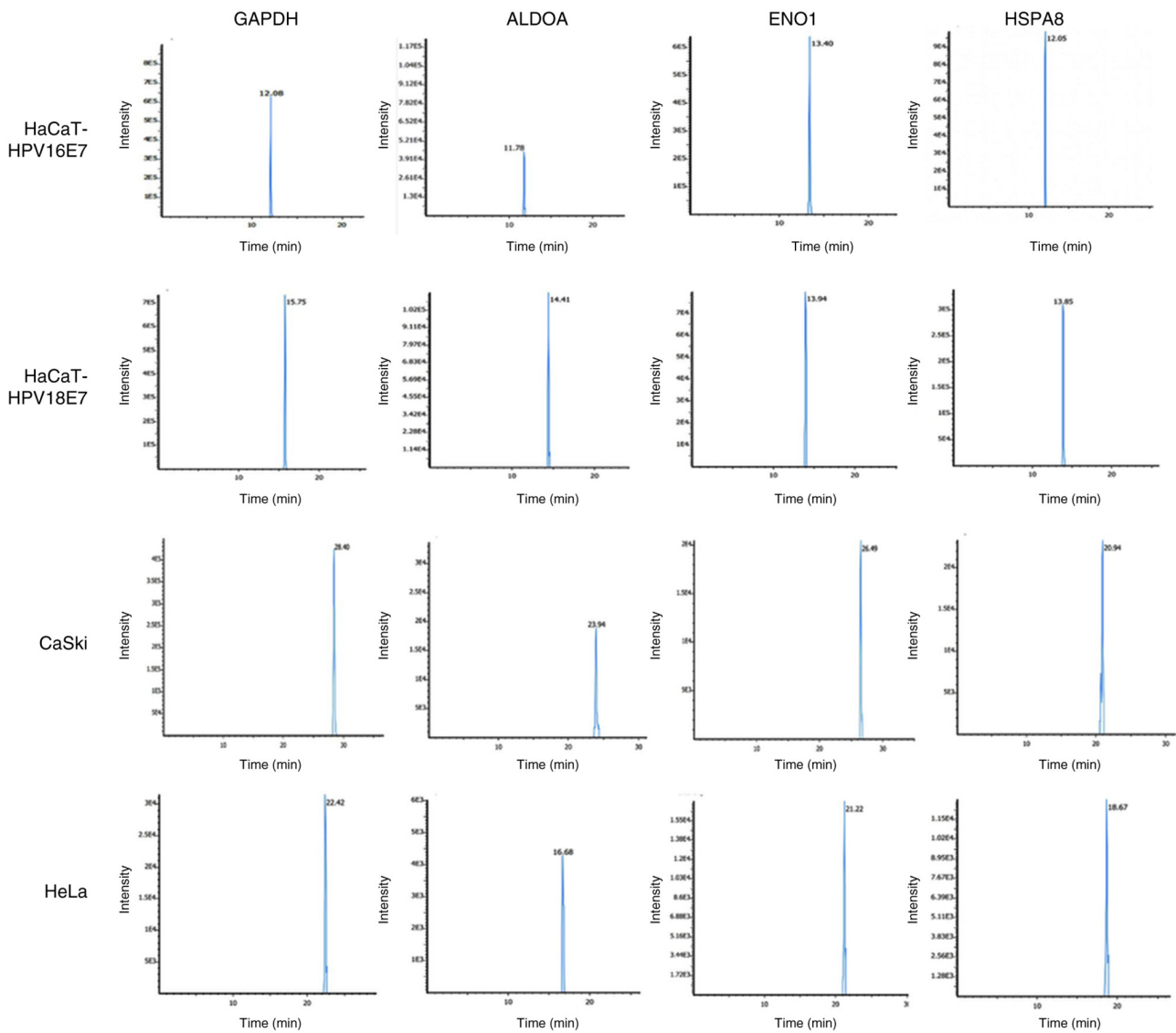


Figure 4. Chromatograms of the proteins corresponding to the liquid chromatography-tandem mass spectrometry analysis of the HPV-transfected (HaCaT-HPV16 E7 and HaCaT-HPV18 E7) and HPV-transformed (CaSki and HeLa) cells. The x-axis represents time (min) while the y-axis represents intensity count. ALDOA, fructose-bisphosphate aldolase; HSPA8, heat shock 70kDa protein 8 isoform 2 variant; HPV human papillomavirus.

most in the entire analysis (GAPDH, PKM, PPIA, HSPD1, ENO1, TUBB4B, EEF2, ANXA2, ANXA1, TUBA1A, ALDOA, NME2, EEFID, ACTN1, MYL6, CFL1, HSPA8 and HNRNPA1). The second-highest number of protein linkages ($n=17$) was demonstrated across all five cell lines (GAPDH, PPIA, HSPD1, ENO1, TUBB4B, EEF2, ANXA2, ANXA1, TUBA1A, ALDOA, NME2, EEFID, ACTN1, MYL6, CFL1, HSPA8 and HNRNPA1). Only two protein linkages, KRT7 and EZR, were demonstrated between HeLa and CaSki cells. The lowest number of protein linkages ($n=1$) was demonstrated in three different groups of linkages as follows: i) HeLa, CaSki, HaCaT control and HaCaT-HPV18 E7; ii) HeLa, CaSki, HaCaT control and HaCaT-HPV16 E7; and iii) HeLa, CaSki, HaCaT-HPV16 E7 and HaCaT-HPV18 E7. The representative chromatograms presented the intensity count for GAPDH, ENO1, ALDOA and HSPA8 proteins with the time taken to pass through the column assessed using the LC-MS/MS analysis of the HPV-transfected (HaCaT-HPV16 E7 and HaCaT-HPV18 E7) and HPV-transformed (CaSki and HeLa) cells (Fig. 4).

Cancer hallmark enrichment of upregulated proteins in HPV-transfected cells. Cancer hallmark enrichment was analyzed based on the P-value and FDR values of the aforementioned upregulated proteins in HaCaT-HPV16/18 E7 cells. The analysis demonstrated that these differentially expressed proteins were significantly enriched across nine pathways (Fig. 5A). A total of 17 of these proteins were involved in the top four enriched pathways: MTORC1 signaling, glycolysis, hypoxia and MYC target VI (Fig. 5B). A total of 10 proteins (PGK1, ALDOA, ENO1, PPIA, GAPDH, HSPD1, PRDX1, PPA1, CCT6A and TXN) were involved with the activation of the mTORC1 complex. A total of seven proteins (PGK1, ALDOA, GAPDH, PRDX1, HSP90AB1, SET and PFN1) were involved with the MYC target VI pathway. Another seven proteins were demonstrated to be involved in cellular response to hypoxia (PGK1, ALDOA, ENO1, PPIA, HSPD1, ANXA2 and EIF4A1). Furthermore, PGK1, ALDOA, ENO1, PPIA, GAPDH, PKM and MYH9 proteins were involved in glycolysis. Notably, PGK1, ALDOA and ENO1 were involved in all

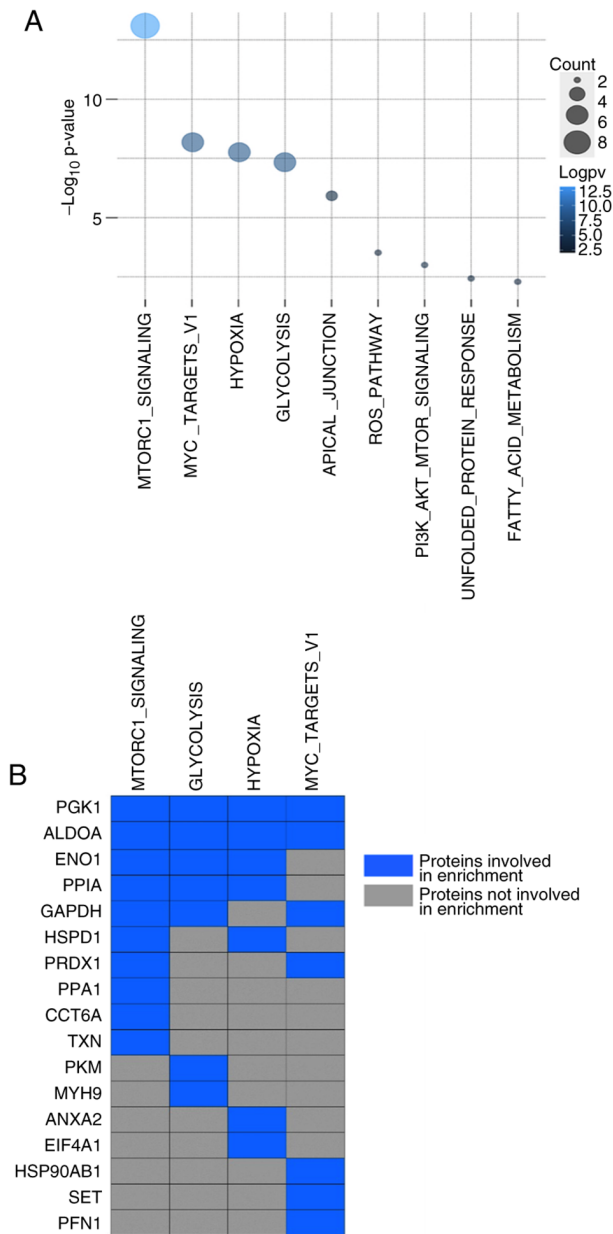


Figure 5. Enrichment analysis delineates cancer hallmarks associated with human papillomavirus transfection in HaCaT-16/18 E7. (A) Cancer hallmark enrichment pathways based on upregulated proteins in human papillomavirus-transfected HaCaT-16/18 E7 cells. Dots represent the protein count in each enrichment pathway. The color represents the log₁₀ p-value of the most significant proteins in the enrichment pathways. (B) Top four cancer hallmark enrichment pathways and their associated proteins. Blue indicates proteins involved in the enrichment pathways and grey indicates proteins not involved in the enrichment pathways. ROS, reactive oxygen species.

four pathways. Other noteworthy cancer hallmark enrichment pathways were apical junction, reactive oxygen species (ROS) pathway, P13K/AKT/mTOR signaling pathway, unfolded protein response and fatty acid metabolism. A total of three proteins (PGK1, ANXA2 and ACTN1) were demonstrated to be engaged in the apical junction pathway. PGK1, PPA1 and PKM were linked to the ROS pathway. PGK1, ACTN1 and EE2 were linked with the PI3K/AKT/mTOR signaling pathway. PGK1, HSP90AB1 and S100A1 were involved with the unfolded protein response, a cellular stress response related to the endoplasmic reticulum. Finally, PGK1, ENO1 and

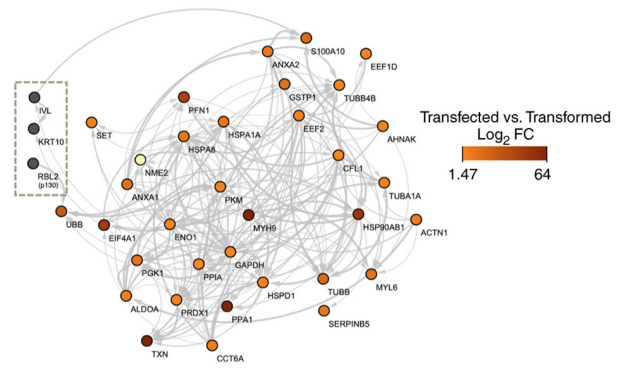


Figure 6. Protein-protein interaction network of upregulated proteins in human papillomavirus-transfected cells. FC, fold change.

HSPA1A were associated with the metabolism of fatty acids. Overall, the results demonstrated that PGK1 expression was upregulated and was involved in all cancer hallmark pathways.

Interactions of upregulated proteins in HPV-transfected cells and HPV-transformed cells with p130, involucrin (IVL) and keratin 10. The upregulated proteins in HPV-transfected and -transformed cells that interacted with p130, IVL and keratin 10 were S100A10, EE2, ANXA2, GSTP1, TUBB4B, EE2, AHNAK, CFL1, TUBA1A, HSP90AB1, ACTN1, PFN1, HSPA1A, HSPA8, PKM, MYH9, SET, NME2, ANXA1, UBB, EIF4A1, ENO1, PGK1, ALDOA, TXN, PRDX1, PPIA, PPA1, CCT6A, GAPDH, HSPD1, TUBB, MYL6 and SERPINB5.

The PPI network for upregulated proteins in HaCaT-HPV16 E7 and HaCaT-HPV18 E7 cells were compared with the target protein network, p130 (also known as RBL2), IVL and keratin 10. p130 was chosen based on its host protein localization, whereas keratin 10 and IVL were selected as protein markers for cellular differentiation. Based on the heat map analysis, PPIs between HPV-transfected and -transformed cells, with their respective log₂ fold changes, were compared. The PPI network demonstrated that p130 only interacted with polyubiquitin-B protein (UBB), which suggested that UBB may be subjected to p130-mediated degradation (Fig. 6). Furthermore, the PPI network also demonstrated that IVL interacted with a calcium-binding protein, S100A10.

GO analysis. All 62 proteins from the LFQ analysis were subjected to functional classification annotation. GO analysis was performed to generate classification clusters in the categories Biological Process (BP), Cellular Component (CC) and Molecular Function (MF). The top upregulated and downregulated differentially expressed proteins linked to BP (Fig. 7A and B), MF (Fig. 7C and D) and CC (Fig. 7E and F) were presented. The subcategories and the number of proteins across 20 GO terms were also labelled. For example, in the BP category, 'cellular process' and 'regulation of biological process' both exceeded 30 upregulated proteins (Fig. 7A), whereas the 'localization' subcategory had eight downregulated proteins (Fig. 7B). In Fig. 7C, top 20 GO terms in the category MF for the upregulated proteins are provided. A high protein count was found in binding and protein binding categories with 34 and 28

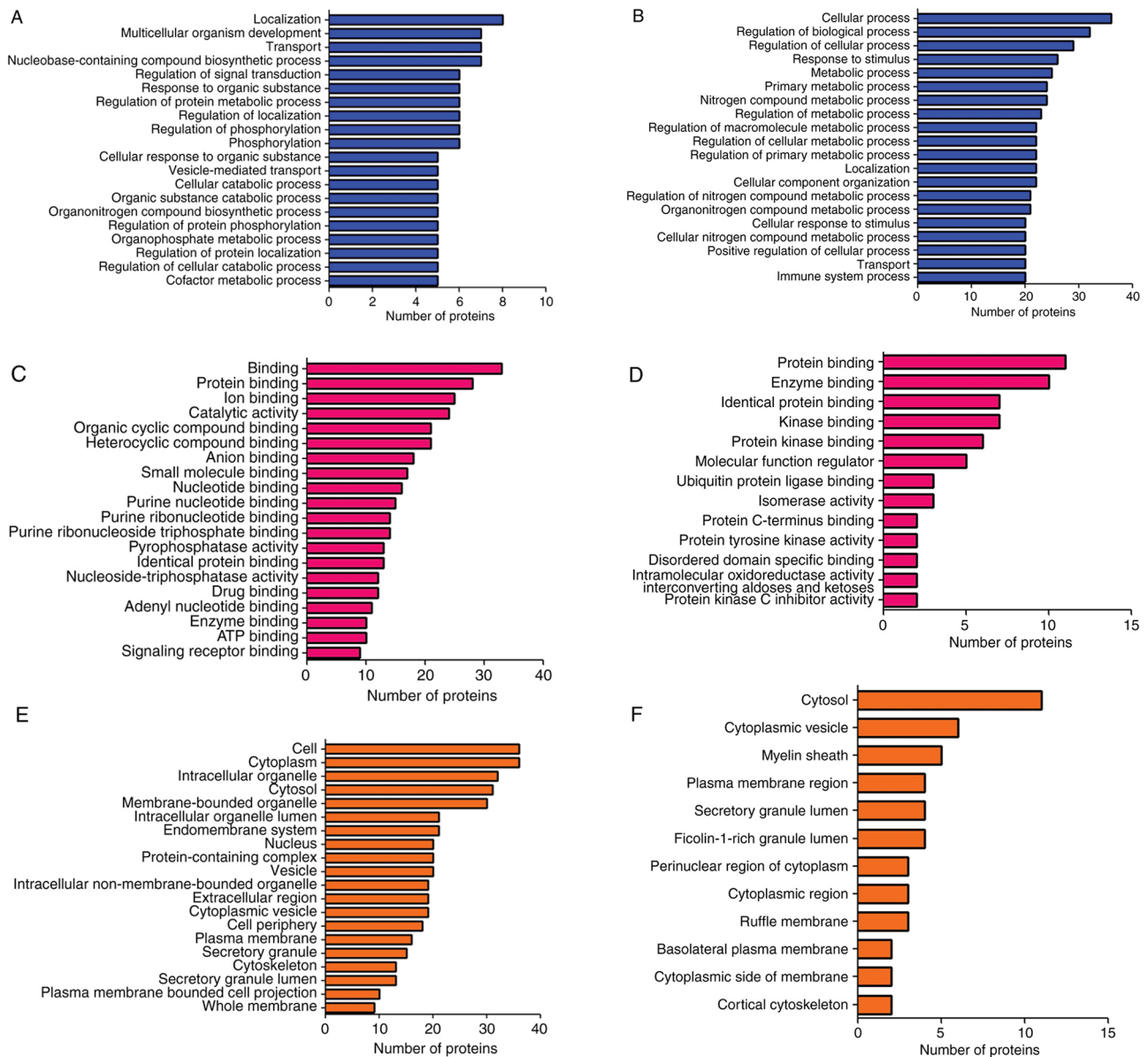


Figure 7. Gene Ontology analysis of (A) upregulated and (B) downregulated differentially expressed proteins in biological process. Gene Ontology analysis of (C) upregulated and (D) downregulated differentially expressed proteins in molecular function. Gene Ontology analysis of (E) upregulated and (F) downregulated differentially expressed proteins in cellular component.

proteins, respectively. The downregulated proteins in MF were enriched in 13 GO terms. Protein and enzyme binding categories had a high protein count with 12 and 11 proteins, respectively (Fig. 7D). The top 20 GO terms corresponding to the CC category for the upregulated proteins are provided in Fig. 7E. Cell and cytoplasm had the highest enrichment with 38 proteins, followed by intracellular organelles, cytosol and membrane-bounded organelle with 30, 31 and 32 proteins, respectively. The downregulated proteins were enriched in 12 GO terms corresponding to CC with the cytosol exhibiting the highest enrichment with 12 proteins, followed by cytoplasmic vesicle with 7 proteins and myelin sheath with 5 proteins (Fig. 7F).

The number of proteins in each subcategory was determined; however, the value must be compared with the actual number of occurrences and the expected number of occurrences for each category to draw a reasonable conclusion.

Discussion

HPV E7 was the first oncogene of all the HPV oncogenes to be identified (15). E7 serves a crucial role in driving cells towards cancer and it may trigger cancer characteristics during the process of viral genome replication. Therefore, HPV E7 gene manipulation may be an effective therapy in CC. Furthermore, transfection of keratinocytes with the HPV E7 oncogene is a suitable model to study the oncogenic changes induced by HPV infection.

In the present study, proteomics technology was used to evaluate the protein expression profiles of HR-HPV E7 types (HPV16 and 18) in HPV-transfected and -transformed cells. HaCaT cells were transfected with recombinant HPV 16/18 E7 and HPV-transformed cells CaSki and HeLa were used to represent native infections with HPV16 and 18, respectively. Label-free proteomics was performed to profile their protein

contents. The results of the present study demonstrated that GPI and ALDOA were common proteins identified in all cell lines, with these proteins being involved in the catalytic activity of glycolysis (37,38). Glycolysis in tumor cells provides energy to support both rapid proliferation and increased metabolic requirements for macromolecule synthesis. GPI is a dimeric enzyme that acts in the second step of glycolysis, where it catalyzes the conversion of glucose-6-phosphate to fructose-6-phosphate (37). Furthermore, it also functions as a cytokine/growth factor induced by c-Myc and HIF-1 (39), and is markedly expressed in numerous types of cancer, such as bladder, colon, stomach, kidney, lung and ovarian cancer, and lymphoma (40). ALDOA functions as a key enzyme catalyzing the reversible reaction of fructose-1,6-bisphosphate to glyceraldehyde-3-phosphate and dihydroxyacetone phosphate in glycolysis. It also serves an essential role in ATP biosynthesis, is ubiquitous in all organs or cells and is upregulated in numerous types of cancer, including cervical adenocarcinoma (41).

The heat map generated based on the LFQ analysis performed in the present study demonstrated that 37 proteins (Cluster 1) were upregulated in HPV-transfected cells compared with in control and HPV-transformed cells. These cluster 1 proteins were further analyzed using volcano plot analysis, which demonstrated that GAPDH, EEF1D, PRDX1, TUBA1A, AHNAK, EEF2, ANXA2, ANXA1, ACTN1, MYL6, SERPINB5, HSPA8, EIF4A1, HSP90AB1 and PFN1 proteins were significantly upregulated in transfected cells. A previous study reported that TUBA1A, PFN1 and ANXA2 proteins were upregulated in cervical squamous cell carcinoma, and HSPA8 and KRT8 were downregulated (42). EEF1D has previously been reported to be upregulated in various types of cancer, such as colorectal carcinoma, esophageal carcinoma, glioblastoma, glioma, liver, lymphoma, medulloblastoma, melanoma, oral squamous cell carcinoma, osteosarcoma, prostate and papillary renal cell carcinoma, thus indicating that the protein may act as a promoter for cell proliferation and tumor growth (43). AHNAK acts as a tumor suppressor via activation of the TGF β /Smad3 signaling cascade, which arrests the cell cycle in the G₀/G₁ phase and downregulates c-Myc expression during cell growth (44). It is closely associated with metastasis of aggressive tumors. A previous study reported unregulated ANXA1 protein expression in cells transfected with HPV16 E6/E7, which suggested its involvement in HPV-mediated carcinogenesis (45). Furthermore, SERPINB5 is differentially expressed in different cancer types. It is upregulated in gastric adenocarcinoma, and breast, colon, gallbladder, ovarian and pancreatic cancer, but downregulated in prostate and gastric cancer (46). SERPINB5 exhibits tumor-suppressive properties due to its nuclear localization, binding to chromatin and inhibiting cancer cell metastasis (47). Overexpression of EIF4A1 has been reported to promote CC progression due to its ATP-dependent RNA helicase activity in mRNA translation of oncoproteins involved in cell apoptosis and proliferation (48). HSP90AB1 is required for cancer cell invasion and migration, and its protein expression levels have been reported to be upregulated in HPV-transfected cells (49).

There were four significant cancer hallmark pathways identified through cancer hallmark enrichment analysis, the mTORC1 signaling pathway, MYC target VI, hypoxia

and glycolysis. The mTORC1 signaling pathway was the prominent hallmark in the present study. In cancer, cells often use the mTOR signaling pathway as a mechanism to enhance their proliferation. mTOR is a Ser/Thr kinase that performs various functions, and is associated with growth (increase in cell mass and size), proliferation, survival, autophagy, metabolism and cytoskeletal organization (50). mTOR activity has been reported to be dysregulated in numerous types of cancer as it serves a vital role in the autophagy of tumor cells. Notably, the inhibitory effect of rapamycin on mTOR activity may increase cell autophagic flux and result in decreased tumor growth. Furthermore, previous studies have demonstrated that rapamycin may promote the formation of autophagosomes and induce autophagosome-lysosome fusion (51,52). Ji and Zheng (53) reported that the mTOR signaling pathway activated cervical carcinoma, and mTOR-specific small interfering RNA was revealed to effectively suppress HeLa cell proliferation via inhibiting the cell cycle and increasing apoptosis, which is similar to the mechanism of action of rapamycin. Rapamycin is a highly specific inhibitor of mTOR that has been used to impede cell proliferation (54). HPV-transfected cells exhibit highly reduced pRB protein expression levels as a consequence of functional E6 and E7 expression (55). It was previously reported that rapamycin resistance in the proliferation of human keratinocytes expressing HPV16 was associated with the ability of E7 to induce pRb degradation. HPV16 E7 was also reported to have conferred resistance to the anti-proliferative effect of rapamycin. This was also associated with the integrity of the LxCxE motif, which has been reported to affect rapamycin resistance (56).

The second significant hallmark was the MYC target VI pathway. MYC is a transcription factor that regulates multiple human genes that promote cell proliferation (57). It also affects apoptosis via alterations to the pro- and anti-apoptotic members of the BCL-2 family, activates telomerase and regulates the expression of vascular endothelial growth factor, which is associated with angiogenesis (58). These downstream targets make MYC one of the most influential oncogenes. Both mTORC1 signaling and MYC target VI (59) are involved in cell proliferation.

The third cancer hallmark was the hypoxia signaling pathway, which is governed by HIF stabilization. While adapting to hypoxia, tumor cells can become more aggressive and become resistant to therapeutics. Hypoxia induces changes to gene expression and the subsequent proteome changes can have notable effects on various functions, which may negatively affect patient prognosis (60). Notably, slowly dividing cells in hypoxic regions are able to escape most cytotoxic drugs, as these treatments target rapidly dividing cells. Cancer stem cells may also be present in poorly hypoxic regions, thus ensuring epithelial-to-mesenchymal transition (61). Tumor cell survival under hypoxia or substances which block HIF-1 α and HIF-2 α -linked signaling pathways makes tumor cells adapt to hypoxia. They do so by inducing metabolic reprogramming, improving the survival of tumor cells, and supporting both angiogenesis and metastasis (62,63). Previous studies have reported that high glucose concentrations (25 mM), which are a common occurrence in the blood of patients with uncontrolled diabetes, may efficiently counteract hypoxic E6/E7

repression. The basis of glucose-linked effects on gene expression is complex, and may involve epigenetic mechanisms and specific transcription factors, such as MondoA/ChREBP-Mlx, NF- κ B, c-Myc and SP1 (64). It is necessary to study how E6/E7 repression under hypoxia influences viral antigen presentation on HPV-positive cancer cells, thereby assisting their escape from host immune defense mechanisms.

Glycolysis was the final cancer hallmark addressed in the present study. Viral proteins regulate the cell cycle via interacting with the tumor suppressor proteins p53 and pRB. HPV E6/E7, as well as E5 and E2, favor the Warburg effect and can contribute to radioresistance and chemoresistance, supporting glycolytic enzyme activities, Krebs cycle and respiratory chain inhibition (65). These processes lead to the accelerated production of ATP, which may satisfy the energy demands of cancer cells during proliferation. In this manner, HPV proteins may promote cancer hallmarks; however, it is also possible that during early HPV infection, the Warburg effect may aid efficient viral replication (66).

The present study demonstrated that PGK1 was present in all cancer hallmark enrichment pathways, which indicated it as a potential biomarker. Previous studies reported that the protein expression levels of PGK1 were elevated in breast cancer (67), astrocytoma (68), metastatic colon cancer (69) and pancreatic ductal adenocarcinoma (70). Furthermore, its mRNA expression levels have been shown to be elevated in gastric cancer (71). PGK1 is an essential enzyme in aerobic glycolysis, which catalyzes the reversible transfer of a phosphate group from 1,3-bisphosphoglycerate to ADP, thus producing 3-phosphoglycerate and ATP. PGK1 can affect the function of some transcription factors, such as β -catenin, a tumor-associated oncoprotein (72). PGK1 is the upstream regulator of β -catenin, which affects tumor growth, proliferation, invasion, metastasis, angiogenesis and drug resistance (69,73,74). Furthermore, PGK1 serves an important role in the tumor occurrence and progression not only as a metabolic enzyme, but also as a protein kinase. Mitochondrial PGK1 activates pyruvate dehydrogenase kinase isoenzyme 1, through which tumor cells are able to inhibit mitochondrial pyruvate metabolism and promote the Warburg effect (75). Abnormal expression of PGK1 has been detected in tumor tissues, and also in peripheral blood and saliva samples of patients (76). Therefore, PGK1 may be considered a potential target for tumor therapy and may become a popular molecule in tumor therapy research. However, the role of PGK1 in different tumors may vary according to its tissue specificity and associated level of expression. Furthermore, the development of therapeutic drugs targeting PGK1 according to its function is also an important consideration. Therefore, PGK1 has a broad research potential in cancer, especially as a therapeutic target for cervical cancer.

The PPI network analysis performed in the present study demonstrated that p130 interacted exclusively with UBB, which is subjected to p130-mediated degradation via proteasomal degradation (77). The UBB protein is part of the ubiquitin-proteasome system (UPS) that is associated with the degradation of various intracellular proteins in eukaryotic cells (78). It is also involved in cellular signaling pathways, such as cell cycle control, cell survival,

proliferation, transcription, DNA repair, apoptosis, cellular metabolism, membrane trafficking and ubiquitination, which are vital for the immune response (79). E7 inactivates most cellular substrates via the interaction of UPS components, leading to their degradation at the proteasome (80). The present study demonstrated that IVL interacted with a calcium-binding protein, S100A10. This protein appears as a small dimeric helix-loop-helix tightly associated with ANXA2 and S100A10 tends to be degraded in the absence of ANXA2. It is involved in the intracellular post-entry trafficking of several membrane-bound proteins (81). It has also been reported to mediate the migration of macrophages to the tumor site (82).

The present study also investigated the functional classification of differentially expressed proteins identified using LFQ analysis to create three distinct clusters: BP, CC and MF. The present study was able to distinguish proteins according to the main clusters affected by HPV infection. Due to its interactions with a wide range of proteins, the effects of E7 were demonstrated across numerous cellular processes, including viral replication, transformation, cell cycle and cell death (83,84). The active site for binding of tumor suppressors with HPV E7 oncoprotein is within conserved region 2, encompassing the LxCxE motif. This motif is responsible for binding with cellular targets. Conserved regions 2 and 3 of HPV are responsible for the degradation of tumor suppressors that ultimately lead to inhibition of cell cycle arrest (85).

In conclusion, developments in HPV research have continued to identify numerous mechanisms that can be exploited by the virus to overcome cellular growth controls. At present, development of accurate therapeutic targets for CC treatment still poses a challenge. The results of the present study demonstrated the importance of elucidating the involvement of multiple pathways perturbed by HPV infection. Furthermore, it was demonstrated that PGK1 was present across all cancer hallmark enrichment pathways. Further investigations are required to identify other PGK1 functions, which could further evaluate its potential as a therapeutic target in CC.

Acknowledgements

Not applicable.

Funding

The present study was supported by the Malaysian Ministry of Higher Education through the Fundamental Research Grant Scheme [grant no. FRGS/1/2016/SKK08/UM/02/16 (FP015-2016)].

Availability of data and materials

The data generated in the present study maybe obtained from the MassIVE database (massive.ucsd.edu) under accession no. MSV000079070. The direct URL is <ftp://massive.ucsd.edu/MSV000090470/>. The datasets were summarized in Tables SI-SVI. The datasets used and/or analyzed during the current study are available from the corresponding author on reasonable request.

Authors' contributions

SG, NFMR, SO, SC and NNR contributed to the conception and design of the present study. Material preparation, data collection and analysis were performed by SG. NNR and MFMR confirm the authenticity of all the raw data. The first draft of the manuscript was written by SG. NNR, MFMR and SO contributed to acquisition of data. SC assisted with data analysis and interpretation. NNR, MFMR, SO and SC critically reviewed the manuscript. All authors have read and approved the final manuscript.

Ethics approval and consent to participate

Not applicable.

Patient consent for publication

Not applicable.

Competing interests

The authors declare that they have no competing interests.

References

- Berman TA and Schiller JT: Human papillomavirus in cervical cancer and oropharyngeal cancer: One cause, two diseases. *Cancer* 123: 2219-2229, 2017.
- Sand FL, Munk C, Jensen SM, Svahn MF, Frederiksen K and Kjaer SK: Long-Term risk for noncervical anogenital cancer in women with previously diagnosed high-grade cervical intraepithelial neoplasia: A danish nationwide cohort study. *Cancer Epidemiol Biomarkers Prev* 25: 1090-1097, 2016.
- Fuller KM and Hinyard L: Factors associated with HPV vaccination in young males. *J Community Health* 42: 1127-1132, 2017.
- Haverkos HW, Haverkos GP and O'Mara M: Co-carcinogenesis: Human papillomaviruses, coal tar derivatives, and squamous cell cervical cancer. *Front Microbiol* 8: 2253, 2017.
- Muñoz N, Bosch FX, De Sanjosé S, Herrero R, Castellsagué X, Shah KV, Snijders PJ and Meijer CJ; International Agency for Research on Cancer Multicenter Cervical Cancer Study Group: Epidemiologic classification of human papillomavirus types associated with cervical cancer. *N Engl J Med* 348: 518-527, 2003.
- Della Fera AN, Warburton A, Coursey TL, Khurana S and McBride AA: Persistent human papillomavirus infection. *Viruses* 13: 321, 2021.
- Songock WK, Kim SM and Bodily JM: The human papillomavirus E7 oncoprotein as a regulator of transcription. *Virus Res* 231: 56-75, 2017.
- Graham SV and Faizo AAA: Control of human papillomavirus gene expression by alternative splicing. *Virus Res* 231: 83-95, 2017.
- Hong HS, Akhavan J, Lee SH, Kim RH, Kang MK, Park NH and Shin KH: Proinflammatory cytokine TNF α promotes HPV-associated oral carcinogenesis by increasing cancer stemness. *Int J Oral Sci* 12: 3, 2020.
- Richards KH, Wasson CW, Watherston O, Doble R, Eric Blair G, Wittmann M and Macdonald A: The human papillomavirus (HPV) E7 protein antagonises an Imiquimod-induced inflammatory pathway in primary human keratinocytes. *Sci Rep* 5: 12922, 2015.
- de Freitas AC, de Oliveira THA, Barros MR Jr and Venuti A: hrHPV E5 oncoprotein: Immune evasion and related immunotherapies. *J Exp Clin Cancer Res* 36: 71, 2017.
- Yeo-The NSL, Ito Y and Jha S: High-risk human papillomaviral oncogenes E6 and E7 target key cellular pathways to achieve oncogenesis. *Int J Mol Sci* 19: 1706, 2018.
- Fischer M, Uxa S, Stanko C, Magin TM and Engeland K: Human papilloma virus E7 oncoprotein abrogates the p53-p21-DREAM pathway. *Sci Rep* 7: 2603, 2017.
- Bienkowska-Haba M, Luszczek W, Zwolinska K, Scott RS and Sapp M: Genome-Wide transcriptome analysis of human papillomavirus 16-infected primary keratinocytes reveals subtle perturbations mostly due to E7 protein expression. *J Virol* 94: e01360-19, 2020.
- Pal A and Kundu R: Human papillomavirus E6 and E7: The cervical cancer hallmarks and targets for therapy. *Front Microbiol* 10: 3116, 2020.
- Cuninghame S, Jackson R and Zehbe I: Hypoxia-inducible factor 1 and its role in viral carcinogenesis. *Virology* 456-457: 370-383, 2014.
- Gunasekharan VK, Li Y, Andrade J and Laimins LA: Post-Transcriptional regulation of KLF4 by high-risk human papillomaviruses is necessary for the differentiation-dependent viral life cycle. *PLoS Pathog* 12: e1005747, 2016.
- Sen P, Ganguly P and Ganguly N: Modulation of DNA methylation by human papillomavirus E6 and E7 oncoproteins in cervical cancer. *Oncol Lett* 15: 11-22, 2018.
- Gandhi S, Nor Rashid N, Mohamad Razif MF and Othman S: Proteasomal degradation of p130 facilitate cell cycle deregulation and impairment of cellular differentiation in high-risk Human Papillomavirus 16 and 18 E7 transfected cells. *Mol Biol Rep* 48: 5121-5133, 2021.
- Schmittgen TD and Livak KJ: Analyzing real-time PCR data by the comparative C(T) method. *Nat Protoc* 3: 1101-1108, 2008.
- Olson BJSC: Assays for determination of protein concentration. *Curr Protoc Pharmacol* 73: A.3A.1-A.3A.32, 2016.
- Tan CH, Tan KY and Tan NH: Revisiting *Notechis scutatus* venom: On shotgun proteomics and neutralization by the 'bivalent' Sea Snake Antivenom. *J Proteomics* 144: 33-38, 2016.
- Zainal Abidin SA, Rajadurai P, Chowdhury ME, Ahmad Rusmili MR, Othman I and Naidu R: Proteomic characterization and comparison of malaysian *tropidolaemus wagleri* and *cryptelytrops purpureomaculatus* venom using shotgun-proteomics. *Toxins (Basel)* 8: 299, 2016.
- Zhang J, Xin L, Shan B, Chen W, Xie M, Yuen D, Zhang W, Zhang Z, Lajoie GA and Ma B: PEAKS DB: de novo sequencing assisted database search for sensitive and accurate peptide identification. *Mol Cell Proteomics* 11: M111.010587, 2012.
- Ma B, Zhang K, Hendrie C, Liang C, Li M, Doherty-Kirby A and Lajoie G: PEAKS: Powerful software for peptide de novo sequencing by tandem mass spectrometry. *Rapid Commun Mass Spectrom* 17: 2337-2342, 2003.
- Levin Y, Schwarz E, Wang L, Leweke FM and Bahn S: Label-free LC-MS/MS quantitative proteomics for large-scale biomarker discovery in complex samples. *J Sep Sci* 30: 2198-2203, 2007.
- Washburn MP, Wolters D and Yates JR Jr: Large-scale analysis of the yeast proteome by multidimensional protein identification technology. *Nat Biotechnol* 19: 242-247, 2001.
- Alsallakh B, Aigner W, Miksch S and Hauser H: Radial sets: Interactive visual analysis of large overlapping sets. *IEEE Trans Vis Comput Graph* 19: 2496-2505, 2013.
- Tyanova S, Temu T, Sinitcyn P, Carlson A, Hein MY, Geiger T, Mann M and Cox J: The Perseus computational platform for comprehensive analysis of (prote)omics data. *Nat Methods* 13: 731-740, 2016.
- Liberzon A, Birger C, Thorvaldsdottir H, Ghandi M, Mesirov JP and Tamayo P: The molecular signatures database (MSigDB) hallmark gene set collection. *Cell Syst* 1: 417-425, 2015.
- Subramanian A, Tamayo P, Mootha VK, Mukherjee S, Ebert BL, Gillette MA, Paulovich A, Pomeroy SL, Golub TR, Lander ES and Mesirov JP: Gene set enrichment analysis: A knowledge-based approach for interpreting genome-wide expression profiles. *Proc Natl Acad Sci USA* 102: 15545-15550, 2005.
- Benjamini Y and Hochberg Y: Controlling the false discovery rate: A practical and powerful approach to multiple testing. *J R Statist Soc B* 57: 289-300, 1995.
- Lin Y, Zhang J, Cai J, Liang R, Chen G, Qin G, Han X, Yuan C, Liu Z, Li Y, *et al*: Systematic analysis of gene expression alteration and co-expression network of eukaryotic initiation factor 4A-3 in cancer. *J Cancer* 9: 4568-4577, 2018.
- Zeng J, He SL, Li LJ and Wang C: Hsp90 up-regulates PD-L1 to promote HPV-positive cervical cancer via HER2/PI3K/AKT pathway. *Mol Med* 27: 130, 2021.
- Shan N, Zhou W, Zhang S and Zhang Y: Identification of HSPA8 as a candidate biomarker for endometrial carcinoma by using iTRAQ-based proteomic analysis. *Onco Targets Ther* 9: 2169-2179, 2016.

36. Potriquet J, Laohaviroj M, Bethony JM and Mulvenna J: A modified FASP protocol for high-throughput preparation of protein samples for mass spectrometry. *PLoS One* 12: e0175967, 2017.
37. Fermo E, Vercellati C, Marcello AP, Zaninoni A, Aytac S, Cetin M, Capolsini I, Casale M, Paci S, Zanella A, *et al*: Clinical and molecular spectrum of glucose-6-phosphate isomerase deficiency. report of 12 new cases. *Front Physiol* 10: 467, 2019.
38. Kawai K, Uemura M, Munakata K, Takahashi H, Haraguchi N, Nishimura J, Hata T, Matsuda C, Ikenaga M, Murata K, *et al*: Fructose-bisphosphate aldolase A is a key regulator of hypoxic adaptation in colorectal cancer cells and involved in treatment resistance and poor prognosis. *Int J Oncol* 50: 525-534, 2017.
39. Zdravčević M, Marchiq I, de Padua MMC, Parks SK and Pouyssegur J: Metabolic plasticity in cancers-distinct role of glycolytic enzymes GPI, LDHs or membrane transporters MCTs. *Front Oncol* 7: 313, 2017.
40. Han J, Deng X, Sun R, Luo M, Liang M, Gu B, Zhang T, Peng Z, Lu Y, Tian C, *et al*: GPI is a prognostic biomarker and correlates with immune infiltrates in lung adenocarcinoma. *Front Oncol* 11: 752642, 2021.
41. Saito Y, Takasawa A, Takasawa K, Aoyama T, Akimoto T, Ota M, Magara K, Murata M, Hirohashi Y, Hasegawa T, *et al*: Aldolase A promotes epithelial-mesenchymal transition to increase malignant potentials of cervical adenocarcinoma. *Cancer Sci* 111: 3071-3081, 2020.
42. Saritha V, Abdul J, Arun S and Meenakshi SK: Analysis of differentially expressed proteins in the exfoliated cells of normal and squamous cell carcinoma of the uterine cervix to define candidate markers for cervical cancer. *Int J Bioc Biotechnol* 5: 626-636, 2016.
43. Xu H, Yu S, Peng K, Gao L, Chen S, Shen Z, Han Z, Chen M, Lin J, Chen S and Kang M: The role of EEF1D in disease pathogenesis: A narrative review. *Ann Transl Med* 9: 1600, 2021.
44. Sohn M, Shin S, Yoo JY, Goh Y, Lee IH and Bae YS: Ahnak promotes tumor metastasis through transforming growth factor- β -mediated epithelial-mesenchymal transition. *Sci Rep* 8: 14379, 2018.
45. Calmon MF, Sichero L, Boccardo E, Villa LL and Rahal P: HPV16 E6 regulates annexin 1 (ANXA1) protein expression in cervical carcinoma cell lines. *Virology* 496: 35-41, 2016.
46. Manawapat-Klopfer A, Thomsen LT, Martus P, Munk C, Russ R, Gmuender H, Frederiksen K, Haedicke-Jarboui J, Stubenrauch F, Kjaer SK and Iftner T: TMEM45A, SERPINB5 and p16INK4A transcript levels are predictive for development of high-grade cervical lesions. *Am J Cancer Res* 6: 1524-1536, 2016.
47. Chang IW, Liu KW, Ragunanan M, He HL, Shiue YL and Yu SC: SERPINB5 Expression: Association with CCRT Response and Prognostic Value in Rectal Cancer. *Int J Med Sci* 15: 376-384, 2018.
48. Liang S, Ju X, Zhou Y, Chen Y, Ke G, Wen H and Wu X: Downregulation of eukaryotic initiation factor 4A1 improves radiosensitivity by delaying DNA double strand break repair in cervical cancer. *Oncol Lett* 14: 6976-6982, 2017.
49. Wang H, Deng G, Ai M, Xu Z, Mou T, Yu J, Liu H, Wang S and Li G: Hsp90ab1 stabilizes LRP5 to promote epithelial-mesenchymal transition via activating of AKT and Wnt/ β -catenin signaling pathways in gastric cancer progression. *Oncogene* 38: 1489-1507, 2019.
50. Saxton RA and Sabatini DM: mTOR signaling in growth, metabolism, and disease. *Cell* 168: 960-976, 2017.
51. Rezazadeh D, Norooznezhad AH, Mansouri K, Jahani M, Mostafaie A, Mohammadi MH and Modarressi MH: Rapamycin reduces cervical cancer cells viability in hypoxic condition: Investigation of the role of autophagy and apoptosis. *Oncotargets Ther* 13: 4239-4247, 2020.
52. Dossou AS and Basu A: The emerging roles of mTORC1 in macromanaging autophagy. *Cancers (Basel)* 11: 1422, 2019.
53. Ji J and Zheng PS: Activation of mTOR signaling pathway contributes to survival of cervical cancer cells. *Gynecol Oncol* 117: 103-108, 2010.
54. Lamming DW: Inhibition of the mechanistic target of rapamycin (mTOR)-rapamycin and beyond. *Cold Spring Harb Perspect Med* 6: a025924, 2016.
55. Yim EK and Park JS: The role of HPV E6 and E7 oncoproteins in HPV-associated cervical carcinogenesis. *Cancer Res Treat* 37: 319-324, 2005.
56. Rabachini T, Boccardo E, Andrade R, Perez KR, Nonogaki S, Cuccovia IM and Villa LL: HPV-16 E7 expression up-regulates phospholipase D activity and promotes rapamycin resistance in a pRB-dependent manner. *BMC Cancer* 18: 485, 2018.
57. Chanvorachote P, Sriratanasak N and Nonpanya N: C-myc contributes to malignancy of lung Cancer: A potential anticancer drug target. *Anticancer Res* 40: 609-618, 2020.
58. Xu J, Chen Y and Olopade OI: MYC and breast cancer. *Genes Cancer* 1: 629-640, 2010.
59. Meyer N and Penn LZ: Reflecting on 25 years with MYC. *Nat Rev Cancer* 8: 976-990, 2008.
60. Roma-Rodrigues C, Mendes R, Baptista PV and Fernandes AR: Targeting tumor microenvironment for cancer therapy. *Int J Mol Sci* 20: 840, 2019.
61. Shibue T and Weinberg RA: EMT, CSCs, and drug resistance: The mechanistic link and clinical implications. *Nat Rev Clin Oncol* 14: 611-629, 2017.
62. Balamurugan K: HIF-1 at the crossroads of hypoxia, inflammation, and cancer. *Int J Cancer* 138: 1058-1066, 2016.
63. Semenza GL: Hypoxia-inducible factors: Mediators of cancer progression and targets for cancer therapy. *Trends Pharmacol Sci* 33: 207-214, 2012.
64. Havula E and Hietakangas V: Glucose sensing by ChREBP/MondoA-Mlx transcription factors. *Semin Cell Dev Biol* 23: 640-647, 2012.
65. Martínez-Ramírez I, Carrillo-García A, Contreras-Paredes A, Ortiz-Sánchez E, Cruz-Gregorio A and Lizano M: Regulation of cellular metabolism by high-risk human papillomaviruses. *Int J Mol Sci* 19: 1839, 2018.
66. Medda A, Duca D and Chiocca S: Human papillomavirus and cellular pathways: Hits and targets. *Pathogens* 10: 262, 2021.
67. Zhang D, Tai LK, Wong LL, Chiu LL, Sethi SK and Koay ES: Proteomic study reveals that proteins involved in metabolic and detoxification pathways are highly expressed in HER-2/neu-positive breast cancer. *Mol Cell Proteomics* 4: 1686-1696, 2005.
68. Yan H, Yang K, Xiao H, Zou YJ, Zhang WB and Liu HY: Over-expression of cofilin-1 and phosphoglycerate kinase 1 in astrocytomas involved in pathogenesis of radioresistance. *CNS Neurosci Ther* 18: 729-736, 2012.
69. Ahmad SS, Glatzle J, Bajaeifer K, Bühler S, Lehmann T, Königsrainer I, Vollmer JP, Sipos B, Ahmad SS, Northoff H, *et al*: Phosphoglycerate kinase 1 as a promoter of metastasis in colon cancer. *Int J Oncol* 43: 586-590, 2013.
70. Hwang TL, Liang Y, Chien KY and Yu JS: Overexpression and elevated serum levels of phosphoglycerate kinase 1 in pancreatic ductal adenocarcinoma. *Proteomics* 6: 2259-2272, 2006.
71. Zieker D, Königsrainer I, Tritschler I, Löffler M, Beckert S, Traub F, Nieselt K, Bühler S, Weller M, Gaedcke J, *et al*: Phosphoglycerate kinase 1 a promoting enzyme for peritoneal dissemination in gastric cancer. *Int J Cancer* 126: 1513-1520, 2010.
72. Rojas-Pirela M, Andrade-Alviárez D, Rojas V, Kemmerling U, Cáceres AJ, Michels PA, Concepción JL and Quiñones W: Phosphoglycerate kinase: Structural aspects and functions, with special emphasis on the enzyme from Kinetoplastea. *Open Biol* 10: 200302, 2020.
73. Lowy AM, Clements WM, Bishop J, Kong L, Bonney T, Sisco K, Aronow B, Fenoglio-Preiser C and Groden J: β -Catenin/Wnt signaling regulates expression of the membrane type 3 matrix metalloproteinase in gastric cancer. *Cancer Res* 66: 4734-4741, 2006.
74. Yamada T, Takaoka AS, Naishiro Y, Hayashi R, Maruyama K, Maesawa C, Ochiai A and Hirohashi S: Transactivation of the multidrug resistance 1 gene by T-cell factor 4/ β -catenin complex in early colorectal carcinogenesis. *Cancer Res* 60: 4761-4766, 2000.
75. Li X, Jiang Y, Meisenhelder J, Yang W, Hawke DH, Zheng Y, Xia Y, Aldape K, He J, Hunter T, *et al*: Mitochondria-translocated PGK1 functions as a protein kinase to coordinate glycolysis and the TCA cycle in tumorigenesis. *Mol Cell* 61: 705-719, 2016.
76. Yu X and Li S: Non-metabolic functions of glycolytic enzymes in tumorigenesis. *Oncogene* 36: 2629-2636, 2017.
77. Kalejta RF and Shenk T: Proteasome-dependent, ubiquitin-independent degradation of the Rb family of tumor suppressors by the human cytomegalovirus pp71 protein. *Proc Natl Acad Sci USA* 100: 3263-3268, 2003.
78. Schwartz AL and Ciechanover A: Targeting proteins for destruction by the ubiquitin system: Implications for human pathobiology. *Annu Rev Pharmacol Toxicol* 49: 73-96, 2009.
79. Đukić A, Lulić L, Thomas M, Skelin J, Bennett Saidu NE, Grce M, Banks L and Tomaić V: HPV oncoproteins and the ubiquitin proteasome system: A signature of malignancy? *Pathogens* 9: 133, 2020.

80. Gupta I, Singh K, Varshney NK and Khan S: Delineating crosstalk mechanisms of the ubiquitin proteasome system that regulate apoptosis. *Front Cell Dev Biol* 6: 11, 2018.
81. Taylor JR, Skeate JG and Kast WM: Annexin A2 in virus infection. *Front Microbiol* 9: 2954, 2018.
82. Xia C, Braunstein Z, Toomey AC, Zhong J and Rao X: S100 proteins as an important regulator of macrophage inflammation. *Front Immunol* 8: 1908, 2018.
83. McLaughlin-Drubin ME, Huh KW and Munger K: Human papillomavirus type 16 E7 oncoprotein associates with E2F6. *J Virol* 82: 8695-8705, 2008.
84. McLaughlin-Drubin ME, Meyers J and Munger K: Cancer associated human papillomaviruses. *Curr Opin Virol* 2: 459-466, 2012.
85. Aarthy M and Singh SK: Interpretations on the interaction between protein tyrosine phosphatase and E7 oncoproteins of high and low-risk HPV: A computational perception. *ACS Omega* 6: 16472-16487, 2021.